ROCK PHYSICS INVERSION WORKFLOW ON RESERVOIR PARAMETERS: A CASE STUDY OF SEISMIC HYDROCARBON DETECTION IN LARGE-AREA TIGHT DOLOMITE RESERVOIRS

ZHAOBING HAO[1], JING BA[2*], LIN ZHANG[3], QINGCAI ZENG[4], REN JIANG[4], JIONG LIU[5], WEI QIAN[2], WENHUI TAN[2] and WEI CHENG[2]

[1] *Key Laboratory of Petroleum Resource Research, Institute of Geology and Geophysics, Chinese Academy of Sciences, Beijing 100029, P.R. China.*
[2] *Institute of Earth Probe, School of Earth Sciences and Engineering, Hohai University, Nanjing. 211100, P.R. China. jba@hhu.edu.cn*
[3] *China University of Petroleum (Beijing), Karamay 834000, P.R. China.*
[4] *Research Institute of Petroleum Exploration and Development - Langfang, CNPC, Langfang. 065007, P.R. China.*
[5] *Center of Geophysical Research for Petroleum, SINOPEC, Beijing 100083, P.R. China.*

(Received May 27, 2016; revised version accepted October 8, 2016)

ABSTRACT

Hao, Z., Ba, J., Zhang, L., Zeng, Q., Jiang, R., Liu, J., Qian, W, Tan, W. and Cheng, W., 2016. Rock physics inversion workflow on reservoir parameters: A case study of seismic hydrocarbon detection in large-area tight dolomite reservoirs. *Journal of Seismic Exploration*, 25: 561-588.

Lateral heterogeneities of the geological characteristics in hydrocarbon reservoirs pose a major challenge for the wide application of rock physics modeling and relevant hydrocarbon detection techniques. In the application of 3D seismic inversion in a large work area, studies on improving hydrocarbon seismic prediction accuracy by effectively utilizing multiple-well log data and multi-scale wave responses is still a hotspot and difficulty in the research area of quantitative seismic interpretation. By combining the rock physics model with the pre-stack seismic inversion, quantitative estimate of reservoir properties can be performed. However, due to the different observation scales of seismic, well log and laboratory observation, the rock physics model established at each scale is different and the data between different scales cannot be effectively related in a combined application. This paper probes into the dolomite gas reservoirs with low porosity and low permeability in the MX work area. We consider the reservoir environment, lithology and pore fluid to predict the wave response dispersions on the basis of poroelasticity theory, and produce the multi-scale rock physics models to relate wave data between different scales.

0963-0651/16/$5.00

By analyzing the models and the well production reports, we adjust the log interpretation results and perform fluid sensitivity analysis on rock physics parameters at acoustic and ultrasonic scales, respectively. Comparison shows that the pattern and sequence of sensitivity parameters from the two scales are basically consistent. The parameters which are the most sensitive to porosity and gas saturation are selected. Based on the single-well rock physics templates which is built in the analysis of each key reference wells, optimization is made to output the standard template for the work area. The standard template takes into account the general geological and petrophysical characteristics of the target stratum. By analyzing the lateral variation and heterogeneity of reservoir geological characteristics in the large work area, the input parameters of rock physics modeling at each well coordinates are adjusted according to the gas production reports, and optimization is made in the 3D work area to establish the 3D data volume of rock physics template. In combination with the pre-stack seismic inversion, the porosity and saturation are estimated in the target stratum, and the estimate results are smoothed to output the final inversion data volume. By comparing with the log interpretation and production testing results, it is proved that the prediction results are correct and the methodology is effective.

KEY WORDS: multi-scale rock physics model, sensitivity parameter, large 3D work area, tight dolomite gas reservoir, pre-stack seismic inversion, porosity and saturation.

INTRODUCTION

At present, the direct reservoir prediction and oil/gas distribution identification by use of the seismic data has become a hotspot in the research area of exploration geophysics. Seismic data are the conclusion from the properties of different aspects of subsurface reservoir rocks. The uncertainty of the inverse problem leads to the non-uniqueness of seismic interpretation and fluid identification. As the bridge connecting the surface-observed seismic data and reservoir rock parameters, seismic rock physics is the theoretical and experimental basis for quantitative interpretation of hydrocarbon reservoirs. The seismic inversion which is driven by rock physics modeling contributes to the accurate understanding on the hydrocarbon characteristics and distribution patterns in reservoir rocks, therefore coping with non-uniqueness and limitations in seismic inversion problems (Yin et al., 2015).

Studies on rock physics can give the quantitative relations between rock elastic parameters and reservoir physical properties and pore fluid parameters, so as to extend the traditional experimental studies of core sample scale to oil field scale, establish the rock physics models at different observation scales (core, well log and seismic) and achieve the comprehensive integration of multiscale and multidisciplinary data (Tang, 2008). Regarding the three observation scales of seismic, sonic and ultrasonic experiment, most geophysicists now attribute the differences of observation results between scales to the wave velocity dispersion phenomena induced by wave-induced fluid flow mechanism. The three types of fluid flow include macro-scale fluid flow mechanism (Gassmann, 1951; Biot, 1956, 1962), grain-scale pore fluid flow mechanism (Mavko and Nur, 1975; Dvorkin and Nur, 1993; Gurevich et al., 2010; Vinci et al., 2014; Papageorgiou and Chapman, 2015) and mesoscale

(larger than the pore size, but much smaller than seismic wavelength) fluid flow mechanism (White, 1975; Pride and Berryman, 2003; Ba et al., 2011, 2012; Sun et al., 2015).

Based on the Biot-Gassmann theory, Russell et al. (2003, 2011) proposed the Russell fluid factor to characterize the pore fluid type of reservoir rocks which can be directly applied in guiding fluid identification. By using the Biot theory, Liu (2014) presented a fluid factor to improve the accuracy of fluid identification. To avoid the uncertainty and non-uniqueness in establishing the fluid factor, elastic parameters are directly inversed based on pre-stack seismic data to assist hydrocarbon identification (Yin et al., 2010; Zong et al., 2011, 2012; Zhang et al., 2014). By considering that the fluid factor is affected by fluid type, rock matrix and pores, Yin et al. (2013) presented a pseudo-fluid modulus by performing a reasonable rotation on the coordinate axis of the Gassmann fluid term and shear modulus, reducing the impact of solid properties (rock matrix, porosity, etc.) on the fluid factor. Zong et al. (2015) proposed the inversion method for directly characterizing pore fluid types, to eliminate the impact of porosity on fluid identification and therefore realize the qualitative prediction of reservoir fluid. The meso-scale and micro-scale local fluid flow mechanism theory is complicated due to the great input number of rock parameters introduced, therefore it is difficult to develop the related fluid factor and the corresponding studies of fluid identification progresses slowly.

Qualitative prediction on reservoirs can be performed based on the fluid factor techniques. Ødegaard and Avseth (2004) and Avseth et al. (2005) used Biot-Gassmann theory to develop the rock physics template for quantitative prediction on hydrocarbon reservoirs. Afterwards, a series of further studies on the application of rock physics template are carried out. Chi and Han (2009) combined elastic parameters with rock physics template to sort out reservoir lithology and fluid property. Based on the seismic rock physics analysis, He et al. (2011) predicted the gas-bearing sandstone reservoirs by establishing the template on elastic parameter cross-plots. Zhang et al. (2015) analyzed the diversity of carbonate reservoir characteristics to present the quantitative interpretation template of rock physics, and quantitatively predicted the reservoir porosity and gas-bearing properties in combination with the inversion data of work area. Based on the lithology and microstructure characteristics of Longmaxi shale formation, Deng et al. (2015) developed the seismic rock physics model, providing the theoretic basis for sweet-spot prediction in shale rocks. Carcione and Avseth (2015) evaluated organic content and hydrocarbon saturation in source rocks and the pressure in the undisturbed formation by developing physics models for argillaceous source rocks. Comprehensively considering the impact of mineral, organic matters and pore fluid, Nicolás-López and Valdiviezo-Mijangos (2016) used the self-consistent theory in their shale rock physics model and the prediction results have been validated in Barnett-1, Fort St. John and Haynesville-1 shale. Based on the Biot-Rayleigh

theory where the mesoscopic scale fluid flow is introduced, Ba et al. (2013a) analyzed the pore fluid distribution characteristics in heterogeneous gas reservoirs, presented the multi-scale rock physics model to establish the quantitative relations between wave responses and lithology and pore fluids at different scales. Yu et al. (2014) estimated the rock porosity and identified reservoir hydrocarbon by rock physics modeling in heterogeneous carbonate reservoirs, where prediction results were in good agreement with the gas production testing reports from different wells.

In view of the complex pore structure and strong lateral heterogeneity in carbonate reservoirs, the conventional rock physics model, which is established based on a single set of pore structure and the calibration with the single-scale wave data, is not applicable to a large 3D work area. This paper studies on the tight dolomite gas reservoirs of the MX district from west China. Firstly, multi-scale rock physics model is built on the basis of comprehensive analysis on dolomite cores, well log data and geologic reports. Secondly, the sonic log data is analyzed and corrected by use of the rock physics model, and the sensitivity on pore fluids of rock physics parameters is analyzed at the sonic log and ultrasonic scales. The parameters which are the most sensitive to porosity and gas saturation are selected. The single-well rock physics model is given at each well, and the results are optimized to establish the standard rock physics template for the whole 3D work area. In consideration of lateral heterogeneities of reservoir geological characteristics, 3D data volume of rock physics model is formulated in large work area. In combination with seismic inversion, the rock parameters of the target stratum are quantitatively estimated.

OVERVIEW OF WORK AREA AND TECHNICAL WORKFLOW

The MX work area is located within the gentle folded belt in the center of the Sichuan Basin, southwest China. According to the structure, it belongs to the NE-SW Leshan-Longnusi palaeohigh with a total area of about 2330 km^2. The studies on the sedimentary facies indicate the sedimentation of epicontinental sea carbonate platform and the ancient water body is generally shallow. Developed with the large-area grain beach, its geology characteristics is mainly controlled by the ancient landform of sedimentation, sea level change and ancient water depth. The target stratum contains carbonate reservoirs with a thickness of 70-100 m. The reservoir is distributed and developed in a large-area and zonal pattern around the main palaeohigh grain beach (Jin et al., 2014).

The data of core analysis, geology and logging, etc. indicate that the target formation L mainly contains dolomite. In a few layers a small amount of sandy dolomite, limestone and mudstone can be observed. In some local area some pyrite and bitumen are distributed. The dolomite of the target formation

mainly includes the grain and clastic dolomite and a little amount of algal dolomite, sandy dolomite and oolitic dolomite. Reservoir spaces are diversified and the pores have strong heterogeneity, where the intergranular dissolution pores, intercrystalline dissolution pores and caves are developed (as is shown in Fig. 1). The range of the reservoir porosity is 0.02-0.06 and that of the permeability is 0.001×10^{-3} – 0.1×10^{-3} μm^2 (Yang, 2015). The pore fluid types in reservoir are mainly natural gas and brine.

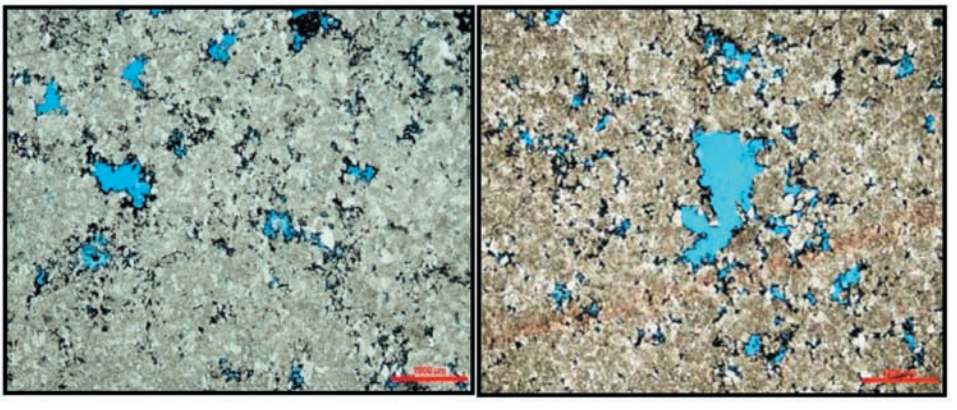

(a) Well MX12, 4651.74-4651.83 m (b) Well MX17, 4612.5-4612.61 m

Fig. 1. Results of the core thin-section analysis of the L-formation in the MX area.

This paper performs rock physics modeling regarding the tight dolomite of the L-formation, and the quantitative prediction is made for porosity and gas saturation in the 3D work area. The specific procedure is shown in Fig. 2. Firstly, the multi-scale rock physics model (Ba et al., 2012; Yu et al., 2014) is produced based on the data from each single well, and the accuracy of the initial model is controlled with respect to log data. After the single-well modeling, models from multiple wells are analyzed in combination, and the standard model for the formation of the whole area is established. The general rock physics characteristics of the formation are described. Fluid sensitivity analysis on the multi-scale rock physics parameters are performed. Finally, the model is calibrated in comparison with gas production testing reports of those known wells and on the basis of seismic data to obtain the 3D rock physics model data volume through an optimization in the whole 3D area, which is applied for the quantitative inversion of reservoir parameters.

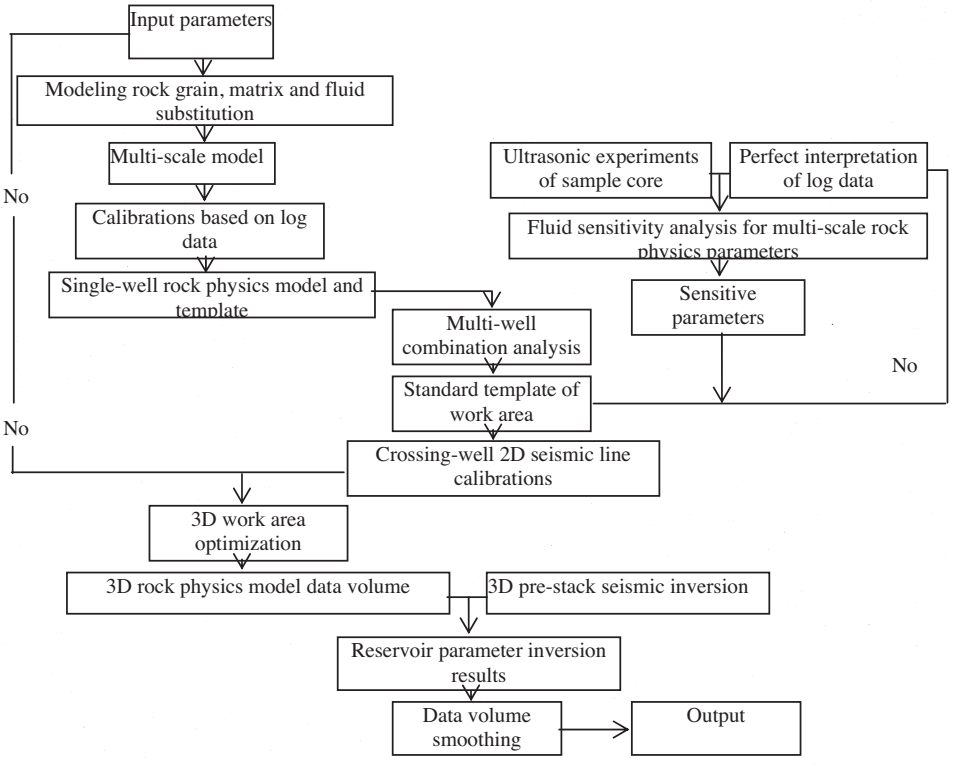

Fig. 2. Flow chart of the rock physics modeling and parameter inversion workflow for the large-area tight reservoirs.

MULTI-SCALE ROCK PHYSICS MODELING

Since the mineral content, pore structure and stratum environment all effect on wave response characteristics, the dolomite rock physics model is developed in a comprehensive analysis of reservoir environments (temperature, pressure), lithology (mineral components, pore shape, shale content and fabric structure) and pore fluid (fluid viscosity and gas/brine patchy-saturation).

Grain elastic modulus

By analyzing the geological data, rock experimental data and log data from the work area, the mineral components and contents of rock are obtained, and then the equivalent elastic modulus of mineral mixture is estimated by use of the Voigt-Reuss-Hill average equation,

$$M_{VRH} = \tfrac{1}{2}[\sum_{i=1}^{N} f_i M_i + (1/\sum_{i=1}^{N} f_i/M_i)] \quad , \tag{1}$$

where M_{VRH} is the grain elastic modulus of mineral mixture, f_i and M_i are the volume content and elastic modulus of the i-th mineral, respectively, and N is the total number of minerals.

Rock matrix elastic modulus

Rock mineral components, pore shape, shale content and pore structure of the reservoir rocks are analyzed, and the bulk and shear moduli of the dry rock skeleton of dolomites are obtained by use of the differential equivalent medium (DEM) theory (Berryman, 1980),

$$(1 - y)d/dy[K^*(y)] = [K_2 - K^*(y)]P^{(*2)}(y) \quad , \tag{2a}$$

$$(1 - y)d/dy[\mu^*(y)] = [\mu_2 - \mu^*(y)]Q^{(*2)}(y) \quad . \tag{2b}$$

The initial condition is $K^*(0) = K_1$ and $\mu^*(0) = \mu_1$, where K_1 and μ_1 are the bulk and shear modulus (phase 1) of the initial principal mineral phase, respectively, and K_2 and μ_2 are the bulk and shear modulus (phase 2) of the inclusion mineral which is gradually inserted into the host phase. y is the content of phase 2 and $P^{(*2)}$ and $Q^{(*2)}$ are related to the shape of the embedded inclusions.

Fig. 3 shows the curves of the moduli of dolomites which contains the coin-shape pores with different aspect ratio (a) and is calculated by the DEM method. The skeleton modulus increases as the aspect ratio of pore increases at the same porosity, and decreases as the porosity increases at the same aspect ratio.

Multi-scale rock physics model

For the rock in the in-situ environment, the density and bulk modulus of pore fluid are dependent on the temperature and pressure, which may be estimated by the van der Waals equation.

The ultrasonic observation data based on core sampling cannot fully reflect the features of the whole reservoirs, and the investigations based on well log data is also hard to reveal the general view of the whole formations. On the

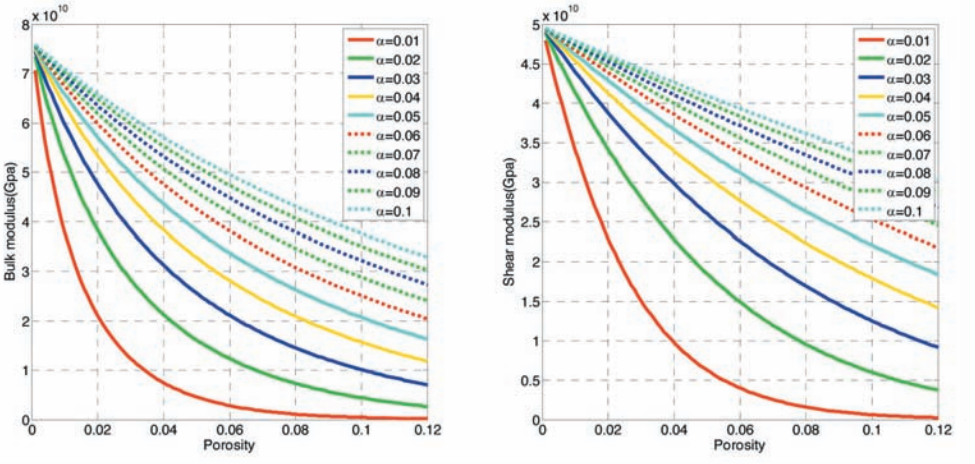

(a) (b)

Fig. 3. Calculation results of the variations of bulk modulus (a) and shear modulus (b) of dolomite skeleton versus porosity.

other hand, seismic survey is not able to probe into the microstructures of reservoir rocks (Tang, 2008). Pore fluid is distributed heterogeneously in the carbonate reservoirs with strong heterogeneities. The classic fluid substitution method with the assumption of a uniform mixture of multi-phase fluids is not appropriate since it cannot reflect the real distribution state of fluid in in-situ rocks. By taking into account the heterogeneous distribution of pore fluid, we neglect the heterogeneity of pore structure and calculate the velocity of P- and S-waves for partially-saturated rocks by use of the Biot-Rayleigh equation (Ba et al., 2012). The effect of elastic wave velocity dispersion versus frequency is predicted so that the multi-scale and multidisciplinary data is integrated in the same model. The Biot-Rayleigh equation is as follows:

$$N\nabla^2\mathbf{u} + (A+N)\nabla e + Q_1\nabla(\xi^{(1)} + \phi_2\varsigma) + Q_2\nabla(\xi^{(2)} - \phi_1\varsigma)$$

$$= \rho_{11}\ddot{\mathbf{u}} + \rho_{12}\ddot{\mathbf{U}}^{(1)} + \rho_{13}\ddot{\mathbf{U}}^{(2)} + b_1(\dot{\mathbf{u}} - \dot{\mathbf{U}}^{(1)}) + b_2(\dot{\mathbf{u}} - \dot{\mathbf{U}}^{(2)}) \quad , \tag{3a}$$

$$Q_1\nabla e + R_1\nabla(\xi^{(1)} + \phi_2\varsigma) = \rho_{12}\ddot{\mathbf{u}} + \rho_{22}\ddot{\mathbf{U}}^{(1)} - b_1(\dot{\mathbf{u}} - \dot{\mathbf{U}}^{(1)}) \quad , \tag{3b}$$

$$Q_2\nabla e + R_2\nabla(\xi^{(2)} - \phi_1\varsigma) = \rho_{13}\ddot{\mathbf{u}} + \rho_{33}\ddot{\mathbf{U}}^{(2)} - b_2(\dot{\mathbf{u}} - \dot{\mathbf{U}}^{(2)}) \quad , \tag{3c}$$

$$\phi_2[Q_1e + R_1(\xi^{(1)} + \phi_2\varsigma)] - \phi_1[Q_2e + R_2(\xi^{(2)} - \phi_1\varsigma)]$$

$$= \tfrac{1}{3}\rho_{f1}\ddot{\varsigma}R_0^2(\phi_1^2\phi_2\phi_{20}/\phi_{10}) + \tfrac{1}{3}(\eta_1\phi_1^2\phi_2\phi_{20}/\kappa)\dot{\varsigma}R_0^2 \quad , \tag{3d}$$

where $\mathbf{u} = [u_1,u_2,u_3]$, $\mathbf{U}^{(1)} = [U_1^{(1)},U_2^{(1)},U_3^{(1)}]$ and $\mathbf{U}^{(2)} = [U_1^{(2)},U_2^{(2)},U_3^{(2)}]$ represent the space vector of displacement of the three components (rock skeleton, fluid 1 and fluid 2), respectively, and the subscript 1, 2 and 3 represent the three major axes in vector space. ς refers to the local fluid flow deformation increments induced by the process of seismic wave propagation. e_{ij}, $\xi_{ij}^{(1)}$ and $\xi_{ij}^{(2)}$ are as follows:

$$e_{ij} = \tfrac{1}{2}[(\partial u_i/\partial x_j) + (\partial u_j/\partial x_i)] \ ,$$

$$\xi_{ij}^{(1)} = \tfrac{1}{2}[(\partial U_i^{(1)}/\partial x_j) + (\partial U_j^{(1)}/\partial x_i)]\delta_{ij} \ ,$$

$$\xi_{ij}^{(2)} = \tfrac{1}{2}[(\partial U_i^{(2)}/\partial x_j) + (\partial U_j^{(2)}/\partial x_i)]\delta_{ij} \ ,$$

where x_2 and x_3 refer to the coordinates at the three axes, respectively. ϕ_1 and ϕ_2 are the absolute porosities of the two types of pores. The total porosity of rock $\phi = \phi_1 + \phi_2$. ϕ_{10} and ϕ_{20} are the local porosities in the two areas, respectively. If the rock only contains one type of skeleton, but saturated with two immiscible fluids, $\phi_{10} = \phi_{20} = \phi$. If ϕ_1 represents water-saturated pores (background/host phase fluid) and ϕ_2 represents gas-saturated pores (inclusion/patchy phase fluid), ϕ_1/ϕ is the water saturation and ϕ_2/ϕ is the gas saturation. ρ_{f1} and η_1 refer to the density and viscosity of host fluid, and ρ_{f2} and η_2 refer to the density and viscosity of inclusion phase fluid. R_0 refers to the gas pocket radius, and κ_{10} refers to the rock permeability. The mathematic determination equations of the elastic parameters A, N, Q_1, R_1, Q_2 and R_2, density parameters ρ_{11}, ρ_{12}, ρ_{13}, ρ_{22} and ρ_{33} and the dissipation parameters b_1 and b_2 are given by Ba et al. (2012).

The mineral mixture modulus and rock skeleton modulus are calculated with the input parameters (rock porosity, clay content and fluid property), and the Biot-Rayleigh equation is solved by the plane wave analytic solution analysis method (Ba et al., 2011) to obtain the P-wave velocity for the water/gas partially-saturated rocks as a function of frequency to derive the quantitative relations between elastic wave responses and rock parameters at different frequencies, i.e., a multi-scale rock physics model.

In this case study, rocks from the target formation are almost pure dolomites with rare clay, where the mineral bulk modulus and density are respectively taken as 76 GPa and 2.87 g/cm^3 of dolomite. By the approach introduced by Ba et al. (2013a, 2013b), the rock skeleton parameters of the formation can be obtained by the calibrations with logging data, the fluid properties are calculated according to the in-situ temperature and pore pressure, and the multiscale rock physics model is produced for quantitative seismic interpretation by use of the Biot-Rayleigh equations. The main parameter of the fluid heterogeneous distribution in the Biot-Rayleigh equations is the gas pocket radius R_0. We determine it by comparing the multiscale theoretical predictions

with those logging data (sonic scale) and experimental data (ultrasonic scale), which is illustrated in Fig. 4. Similar methods for determining the actual fluid distribution parameters or patterns for immiscible fluids in the in-situ rocks have been presented in detail by Caspari et al. (2011) and Ba et al. (2013a).

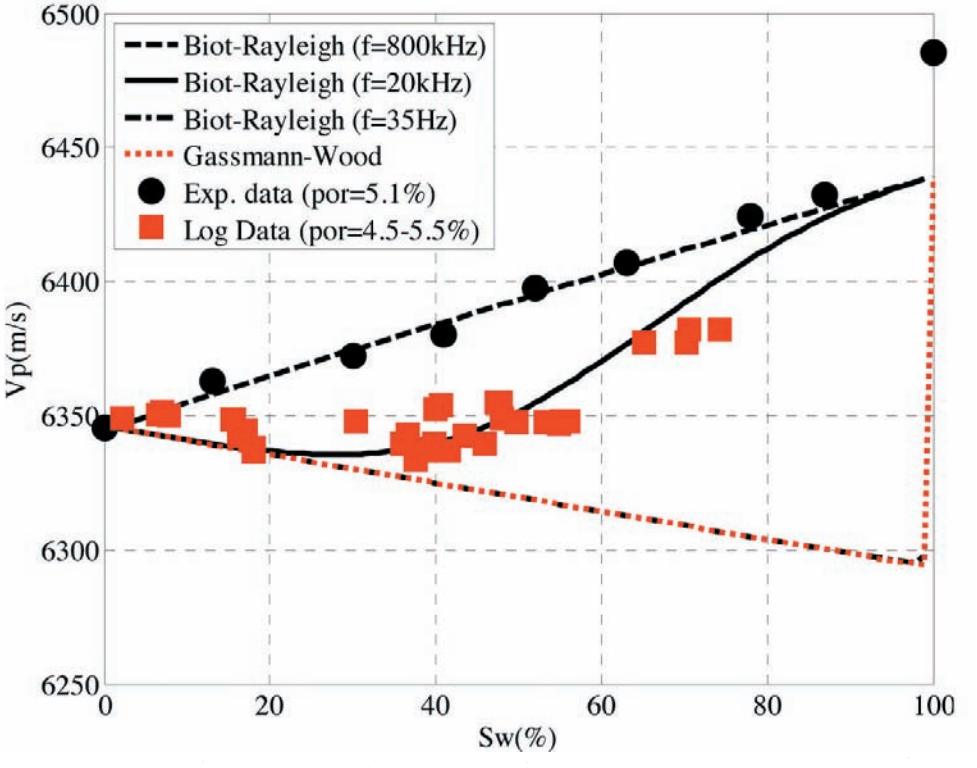

Fig. 4. Compressional wave velocity as a function of brine saturation (S_w) in the comparisons between the Biot-Rayleigh predictions at the ultrasonic, sonic and seismic frequencies and the ultrasonic experimental data and sonic log data from the reservoir rocks.

As is shown in Fig. 4, the ultrasonic experimental measurement of a dolomite specimen with a porosity of 5.1% and the selected sonic log data (in the porosity range of 4.5-5.5%) from in-situ reservoir rocks are compared with those prediction results of the Biot-Rayleigh theory at the seismic (35 Hz), sonic (20 kHz) and ultrasonic (800 kHz) scales. In the ultrasonic test on the partially-saturated rocks we use the experiment set-up as Ba et al. (2016). The sample is partially saturated with nitrogen and brine and the measurement is performed at the confining pressure of 80 MPa and temperature 140° C (the

in-situ condition). The gas saturation in the log data at the sonic scales is obtained by a comprehensive log interpretation. Data are selected from the gas and brine reservoirs at the porosity around 5%, which is used in a comparative analysis with the theoretical predictions to calibrate the in-situ gas pocket size. In theoretical prediction, the rock properties are taken as porosity 5%, permeability 0.09 mD, brine bulk modulus 2.25 GPa, and brine density 1 g/cm^3. The gas pocket size is determined as 0.27 mm by the comparisons, which is almost the twice of the maximum pore/grain size in the sample. The compressional wave velocity as a function of water/brine saturation shows frequency-dependent characteristics. The wave velocity increases with frequency, showing obvious dispersion due to patchy-saturation. The theoretical predictions at different scales agree well with the experimental data and the log data. The ultrasonic measurement at the full brine saturation shows some additional increase of velocity dispersion, which is due to the fabric heterogeneity (Ba et al., 2016).

We also compared the results with the Gassmann theory where the fluids can be mixed homogeneously by using the Wood average, the Gassmann-Wood bound. Although the prediction of Biot-Rayleigh concurs with that of the Gassmann theory at the seismic band, however, it is obviously different with the Gassmann-Wood result at sonic and ultrasonic frequencies. By use of Biot-Rayleigh equations, a unique model for multi-frequency wave data is established, so that the data from different scales can be effectively related to help seismic interpretation.

SINGLE-WELL ROCK PHYSICS MODEL

The well-log curve can be affected by the log instruments, measuring depth, downhole diameter, mud-filtrate invasion and subsurface environments, so the quality of log data shall be evaluated and analyzed before being used for reservoir characterization. After the process of environmental correction, depth alignment, curve editing and normalization, et al. the shale content, porosity and fluid saturation from log data interpretation can be used as the references for calibrating the rock physics model. By combining log data interpretation for hydrocarbon reservoirs and rock physics modeling, the calibrated model can then be applied to predict gas saturation in the stratum (Lv and Sun, 2012).

Fig. 5 shows the cross-plots of the rock physics parameters of log data from well MX204 in the work area. The log curves are edited according to the distribution and dispersion features and by removing outliers. The conclusions of log data interpretation is compared with the actual gas testing reports to carry out the accurate re-interpretation. The porosity and gas saturation from accurate re-interpretation are applied to calibrate the input parameters of rock physics model.

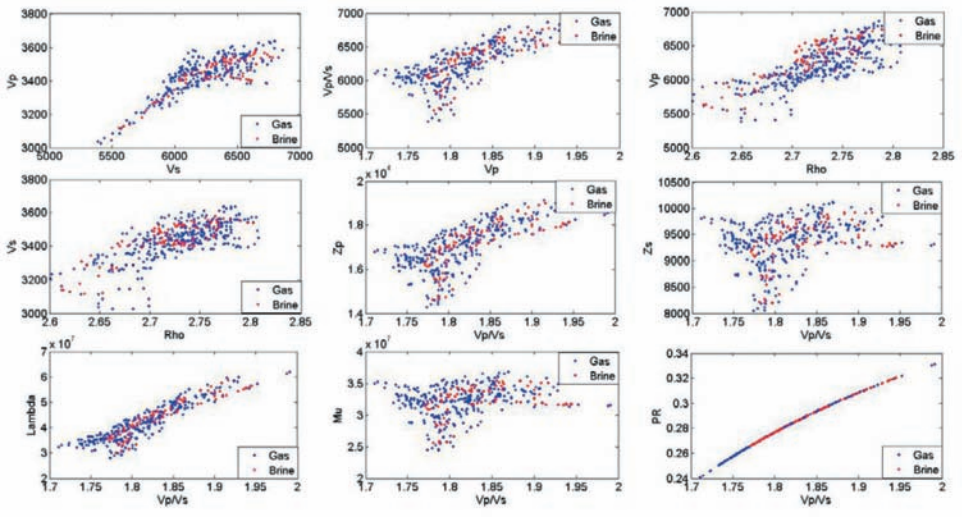

Fig. 5. Cross-plots of the rock physics parameters of well MX204.

The single-well rock physics model is made and calibrated on the basis of edited log data. Fig. 6 and Fig. 7 show the comparison of the rock physics interpretation templates and the log data interpretation results of actual reservoir porosities for well MX9 and MX12, respectively. The comparison indicates that, due to the diversity of carbonate reservoir rocks and the heterogeneity of fluid distribution, the rock physics template obtained based on the single set of pore structures is hard to cover all dispersive data points. In addition, due to the lateral variation of heterogeneity between different wells, each single-well template is different from the others. The model based on the single-well analysis is not capable of representing the high-quality reservoirs of the whole work area. This issue is particularly notable in the actual applications of large-area survey.

FLUID SENSITIVITY ANALYSIS OF ROCK PHYSICS PARAMETERS

Selecting suitable parameters which are the most sensitive to reservoir porosity and gas saturation based on the measured data is very important for the effective application of rock physics models. Since there is difference of wave response data between different scales, the sensitivity analysis of rock physics parameters to reservoir fluids is conducted at each observation scale, respectively.

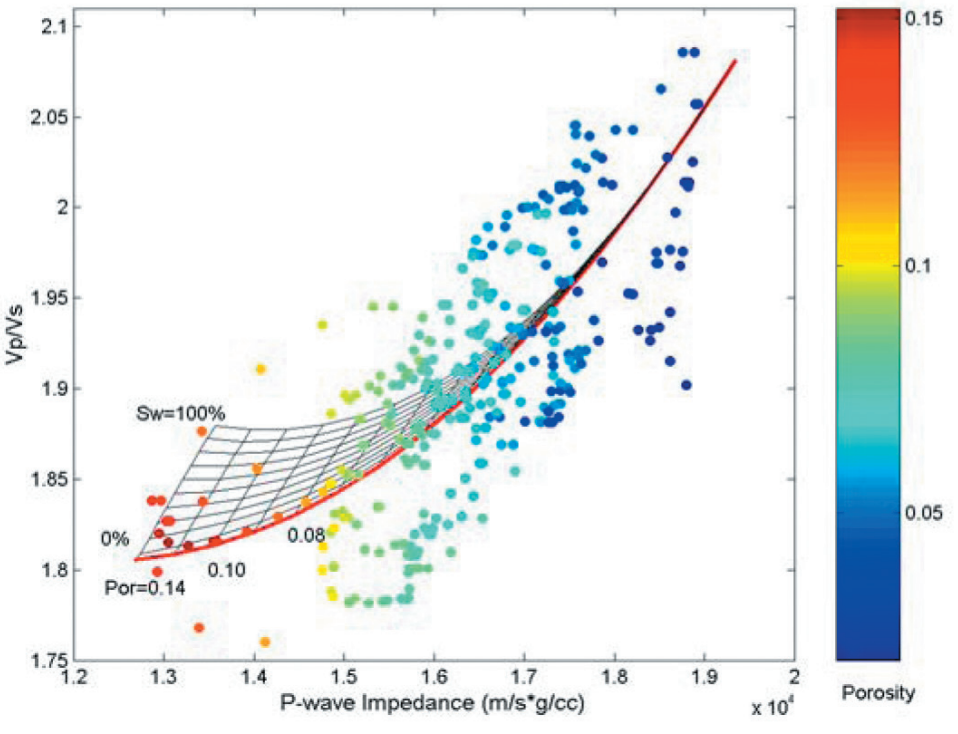

Fig. 6. Rock physics interpretation template of Well MX9.

The sensitivity of rock physics parameters of dolomite to fluid is defined as, the ratio of the difference between the measured water-saturated dolomite parameter A_w and the measured gas-saturated dolomite parameter A_g with A_g, i.e., the relative variation ratio of the measured parameters between different saturation states for the same rock:

$$X = (A_w - A_g)/A_g \quad . \tag{4}$$

At the ultrasonic scale, the 5 dolomite samples are tested under the in-situ reservoir environments (at the confining pressure of 80 MPa and temperature of 140° C). The P-wave and S-wave velocities of core samples are measured at the full saturation of fluids (gas/water) and at the partial saturations of gas and water. Fig. 8 gives the experimental data of the five samples, i.e., the cross-plots of V_P/V_S and P-wave impedance.

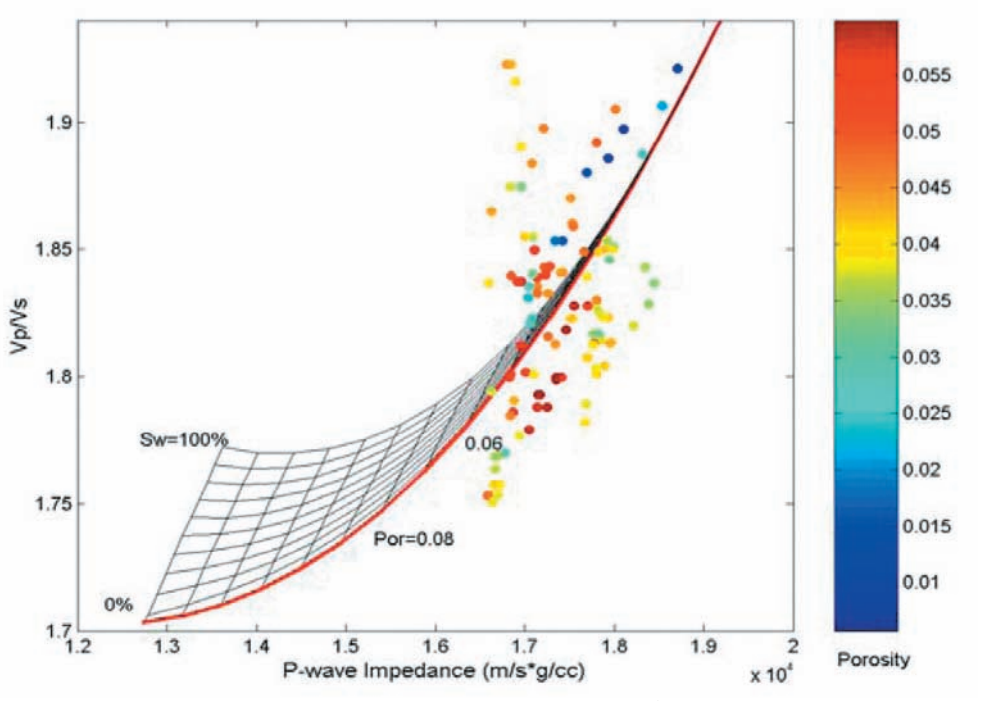

Fig. 7. Rock physics interpretation template of Well MX12.

To investigate the impact of porosity on the rock parameters, the sensitivity of the rock physics parameters and their combinations of the samples at ultrasonic scale are comparatively analyzed based on the measured data of the 5 dolomite samples with porosity 0.051, 0.0534, 0.0547, 0.1208 and 0.1228, respectively. The summary results (see Fig. 9) indicate that, as the porosity decreases, the sensitivity to fluid of each parameter decreases remarkably. There is only slight changes in the sensitivity sequence of rock physics parameters and the basic trend remains unchanged. The parameters of λ and $\lambda\rho$ are the most sensitive to the gas saturation variations and those of μ and V_S are the weakest.

The fluid sensitivity analysis of reservoir rocks at sonic log scale is carried out with the selected seven wells in the work area. By calculating the average value of rock parameters of the water layers and the gas layers from the wells and substituting them to eq. (4), sensitivity at the sonic log scale is estimated. To investigate the sensitivity of rock physics parameters to pore fluid

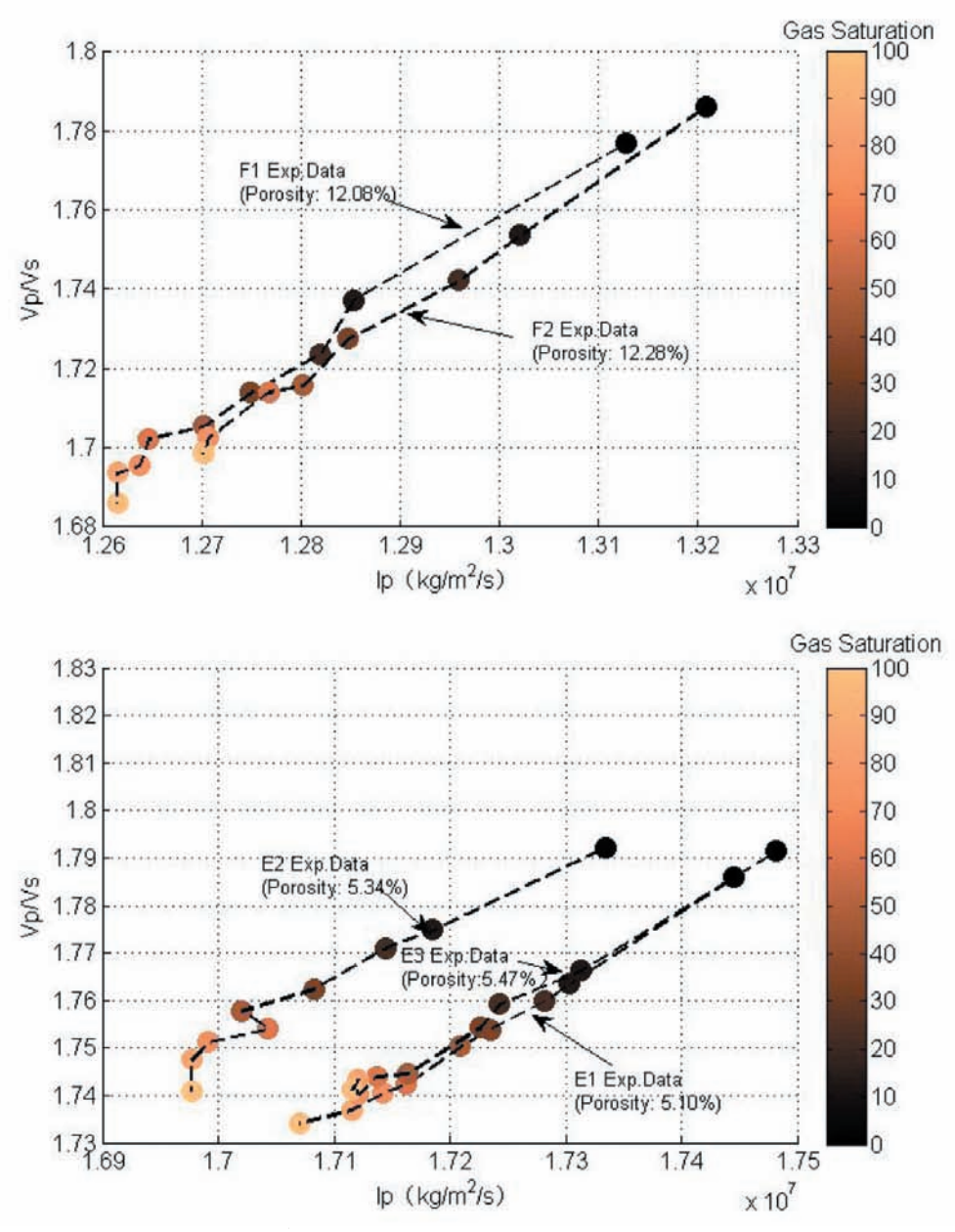

Fig. 8. Cross-plots of V_P/V_S and P-wave impedance for dolomite samples.

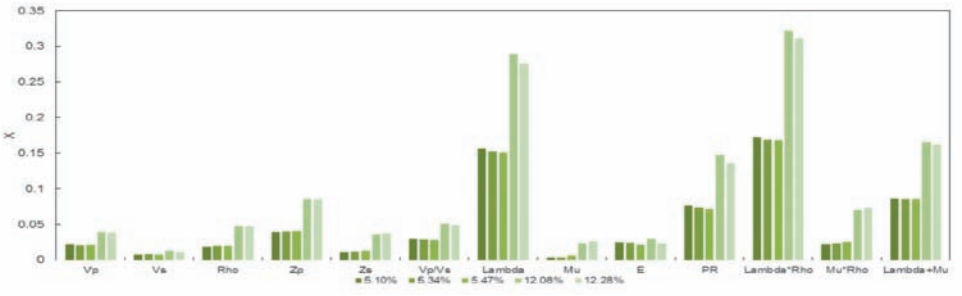

Fig. 9. Fluid sensitivity analysis of the rock physics parameters for the 5 rock samples at ultrasonic scale.

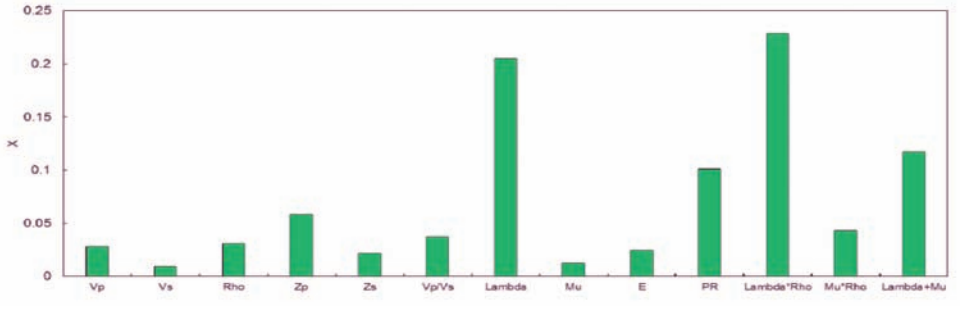

(a) Fluid sensitivity analysis of rock physics parameters at the ultrasonic scale

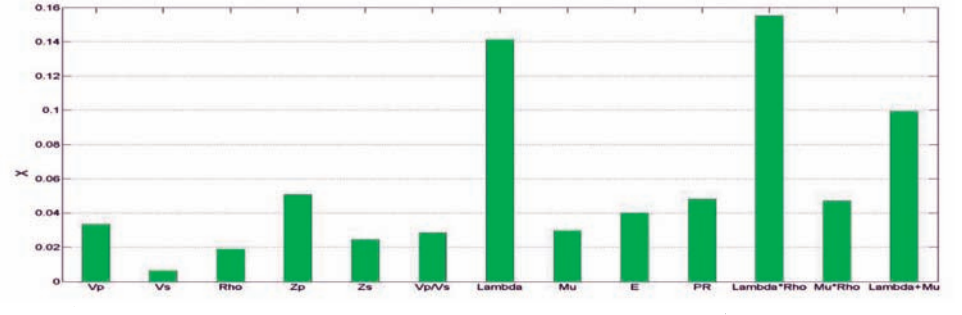

(b) Fluid sensitivity analysis of rock physics parameters at the sonic log scale

Fig. 10. Fluid sensitivity analysis of rock parameters at different observation scales. (a) Fluid sensitivity analysis of rock physics parameters at the ultrasonic scale. (b) Fluid sensitivity analysis of rock physics parameters at the sonic log scale.

at different scales, based on the data of 5 dolomite cores and 7 wells, the sensitivity results at the ultrasonic scale and the sonic log scale are analyzed in comparison, as is shown in Fig. 10.

The comparison indicates that the rock parameters sensitivity features and sequences between the two scales are basically in consistence. The variations of λ and $\lambda\rho$ are the most sensitive to pore fluid changes. The fluid sensitivity of several parameters has slight changes between different observation scales. For example, μ is the least sensitive to pore fluid at the ultrasonic scale, but its sensitivity at the sonic scale is increased. Through a comparative analysis, the selected parameters of λ and $\lambda\rho$ are the most appropriate at the two observation scales, which is the basis for the further reservoir prediction and fluid identification.

STANDARD ROCK PHYSICS TEMPLATE OF THE 3D WORK AREA

In the application of large work area, the single-well rock physics model cannot reflect the general characteristics of geology and seismic response of the target formation. To develop a rock physics model which can describe the general characteristics of the reservoirs, the multi-well observation data and forward modeling must be utilized effectively in a combination analysis. In this paper, several key wells with high gas production which represents the stratum characteristics and mineral components of the work area are selected. Based on the dolomite rock physics model developed at each well, the standard rock physics template for the target formation is produced on the crossplot with the selected sensitivity parameter $\lambda\rho$ and P-wave impedance as the coordinates. The mineral components which are taken into account are dolomite, limestone and clay. Porosity is in range of 0.02-0.12. The fluid types are brine and natural gas. Water saturation is in range of 0-100%.

Each grid point position at the single-well rock physics template can be expressed by $[M_k(i,j), N_k(i,j)]$ according to its coordinates in a 2D cross-plot, where i and j represent the gradual changes of porosity and saturation ($i=1,2,\ldots,11$), corresponds to the gradual change of porosity from 0.02 to 0.12; ($j=1,2,\ldots,11$), corresponds to the gradual change of saturation from 0 to 100%) and k refers to the k-th well. The value $[M_s(i,j), N_s(i,j)]$ at each grid point position of the standard template can be expressed as:

$$M_s(i,j) = \sum_k M_k(i,j) * A(k) * B(i,j) \quad , \tag{5a}$$

$$N_s(i,j) = \sum_k N_k(i,j) * A(k) * C(i,j) \quad , \tag{5b}$$

where A(k) is to the weight of the k-th well. B(i,j), C(i,j), respectively, represent the corrections made to the two coordinates according to the reference data of all wells, at the grid point corresponding to i,j, so as to guarantee the description scope of the template basically cover all the data of key layers from the reference wells.

As is shown in Fig. 11, the log interpretation results are projected onto the calibrated rock physics template. The results indicate that the high water-saturation reservoir rocks from log interpretations and production reports is distributed nearby the water saturation line on the template with the porosity range of 2.8-12%, and the high gas-saturation reservoir rocks from log interpretation and production reports is distributed nearby the full gas saturation line with the porosity range of 3-9.2%. The non-reservoir rocks is distributed in the low-porosity area on the template with the porosity basically lower than 4%. This template generally agrees with the gas testing reports at the target formation of all key wells in the area, reflecting the general characteristics of porosity and fluid distribution of the stratum.

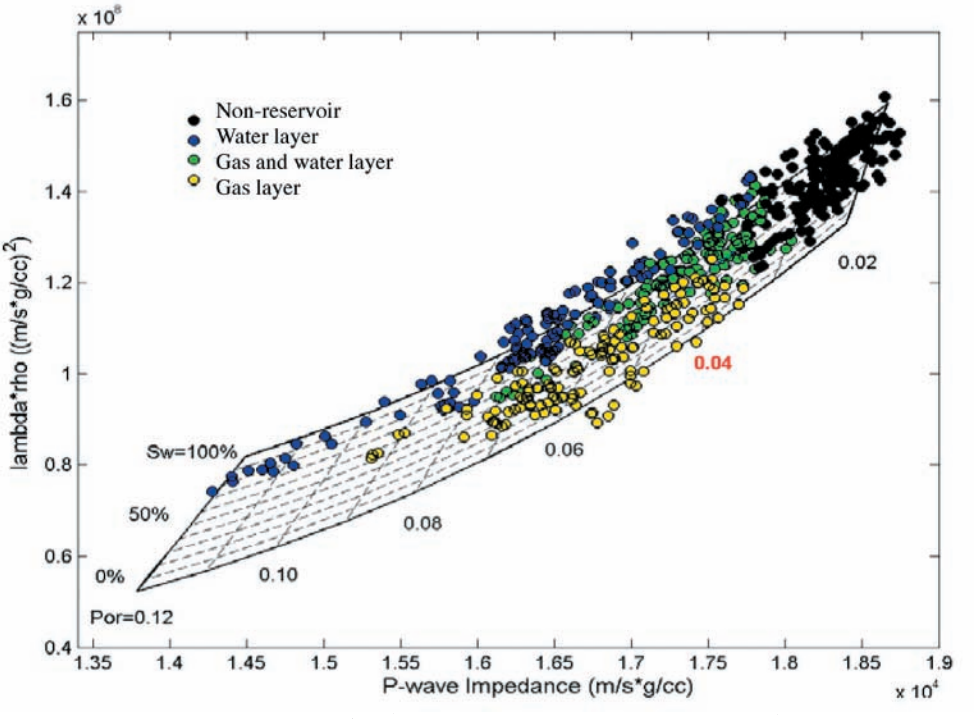

Fig. 11. Cross-plot of the P-wave impedance and $\lambda\rho$ for the work area with the standard rock physics template and the log data points from well MX203, 204, 26 and 27.

ROCK PHYSICS INVERSION ON RESERVOIR PARAMETERS

In the practical application of seismic interpretation and inversion for the standard rock physics template, due to the intrinsic strong heterogeneity of carbonate rocks, the inversion accuracy at different coordinates can be easily affected in a large 3D work area. Therefore, it is essential to perform seismic inversion and fluid detection tests at the position of each well based on the standard template. By extracting 2D crossing-well seismic line from 3D seismic data volume to estimate reservoir and fluid parameters of the target formation near each well location, the results are compared with the known drilling and gas production data of the wells. The template is adjusted to assure inversion results and interpretation conclusion being fully consistent with the known data. The seismic inversion template by debugging the standard template through a 2D seismic inversion tests near the k-th well can be expressed as $[M'_k(i,j), N'_k(i,j)]$.

Optimization based on the seismic inversion template at each well location $[M'_k(i,j), N'_k(i,j)]$ is carried out in the whole work area to produce the 3D data volume of the rock physics model. An independent seismic rock physics model is given at each set of coordinates (x,y) in the area. The determination of its template $[M_{3D}(x,y,i,j), N_{3D}(x,y,i,j)]$ relies on the seismic inversion template at each well location.

$$M_{3D}(x,y,i,j) = \sum_{k=1}^{L} M'_k(i,j) * Q(x,y,k) \quad , \text{ if } x \neq x_k, y \neq y_k, \tag{6a}$$

$$N_{3D}(x,y,i,j) = \sum_{k=1}^{L} N'_k(i,j) * Q(x,y,k) \quad , \text{ if } x \neq x_k, y \neq y_k, \tag{6b}$$

$$M_{3D}(x,y,i,j) = M'_k(i,j) \quad , \text{ if } x \neq x_k, y \neq y_k, \tag{6c}$$

$$N_{3D}(x,y,i,j) = N'_k(i,j) \quad , \text{ if } x \neq x_k, y \neq y_k, \tag{6d}$$

where (x_k,y_k) is the coordinate of the k-th well, L is the total number of the wells and Q(x,y,k) is the weight coefficient of the k-th well which is used for calculating the template at the coordinate (x,y) in the work area. Q(x,y,k) is determined by

$$Q(x,y,k) = \{1/[(x - x_k)^2 + (y - y_k)^2]\} \Big/ \sum_{k'=1}^{L} \{1/[(x - x_{k'})^2 + (y - y_{k'})^2]\} \quad , \text{ if } x \neq x_k, y \neq y_k. \tag{7}$$

Based on eqs. (6) and (7), the observed data at each well are taken into account. Based on the log observation at each geographic position, the seismic inversion and interpretation for reservoir parameters are controlled. The closer spatial distance from the inversion location to a reference well leads to the more remarkable impact from the control of that well. As is shown in Fig. 12, $[M_{3D}(x,y,i,j), N_{3D}(x,y,i,j)]$, i.e., the 3D data volume of rock physics model in the 3D area, is processed along the "xline" direction. In the "inline" direction, each "xline" is processed following the standard seismic data file format of ".sgy".

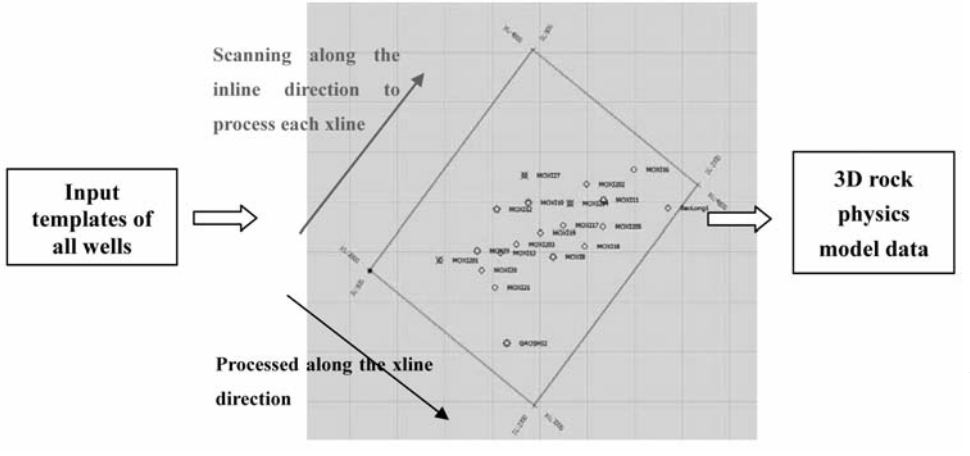

Fig. 12. Schematic diagram for outputting the 3D rock physics model data volume in the work area.

Based on the data volume of rock physics model, 3D seismic data volume for inversion and interpretation is cut and prepared according to the project requirement to perform pre-stack 3D seismic inversion and the inversion for reservoir porosity and hydrocarbon saturation.

SMOOTHING OF INVERSION RESULTS

Based on rock physics modeling, the wave impedance and $\lambda\rho$ from the pre-stack seismic inversion are projected onto the template on the crossplot point by point to sort out the closest grid point on the template, whose porosity and saturation are then the inversed porosity and saturation of the corresponding projected data point (Ba et al., 2013a), so as to predict the hydrocarbon reservoir quality.

In inversing porosity and saturation from seismic data, the uncertainty and non-uniqueness are unavoidable, and the factors of complicated geological structure and seismic processing, etc. may affect the reservoir identification by causing false appearances (Yin et al., 2014). The inversion data of porosity and saturation are smoothed by use of the weighted average method to weaken the impact of the outliers of the inversion/interpretation data. The closer distance to the target position leads to a larger impact from the nearby inversion data. As is shown in eq. (8), Tang (2011) defined the three weighting templates according to the 2D normal distribution. T_1 and T_2 are derived by a 2D Gaussian discrete template and T_3 is the 2D Gaussian template of a 3×3 field. The maximum weight value in the template is the location of the target point.

$$T_1 = (1/9)\begin{pmatrix} 1 & 2 \\ 2 & 4 \end{pmatrix},\quad T_2 = (1/25)\begin{pmatrix} 1 & 1 & 2 \\ 1 & 2 & 4 \\ 2 & 4 & 8 \end{pmatrix},\quad T_2 = (1/16)\begin{pmatrix} 1 & 2 & 1 \\ 2 & 4 & 2 \\ 1 & 2 & 1 \end{pmatrix}. \qquad (8)$$

With T_1 as an example, the 2D inversion section *data(i,j)* is smoothed with the data at the neighboring positions as

$$data_S = \sum_{i,j=1}^{2} data(i,j) * T_1(i,j) \quad , \qquad (9)$$

where $data_S$ is the numerical value at the target position after smoothing. Fig.13 shows the 2D inversion section crossing the well MX8 of the porosity before smoothing, after smoothing and with an enhanced smoothing. The comparison between the data before and after smoothing indicates that the seismic inversion section of porosity is improved in the spatial continuity of the formation.

QUANTITATIVE PREDICTION FOR RESERVOIR HYDROCARBON

The 3D data volume of the rock physics model in combination with the elastic parameter data volume from the pre-stack seismic inversion provides the inversion of rock physics parameters in the 3D work area, therefore the quantitative interpretation of reservoir porosity and hydrocarbon saturation are performed. Fig. 14 shows the horizontal map of the average porosity inversion results of dolomite reservoirs in L formation for a work area larger than 1000km^2. The inversion results show that the reservoirs of the target formation has the characteristics of low porosity, the range of the reservoir average porosity is 0-0.045 and the high-quality reservoirs are mainly distributed in the middle zone of the work area, where is the structural high position. Fig. 15 shows the average gas saturation results in the reservoir rocks, which indicate

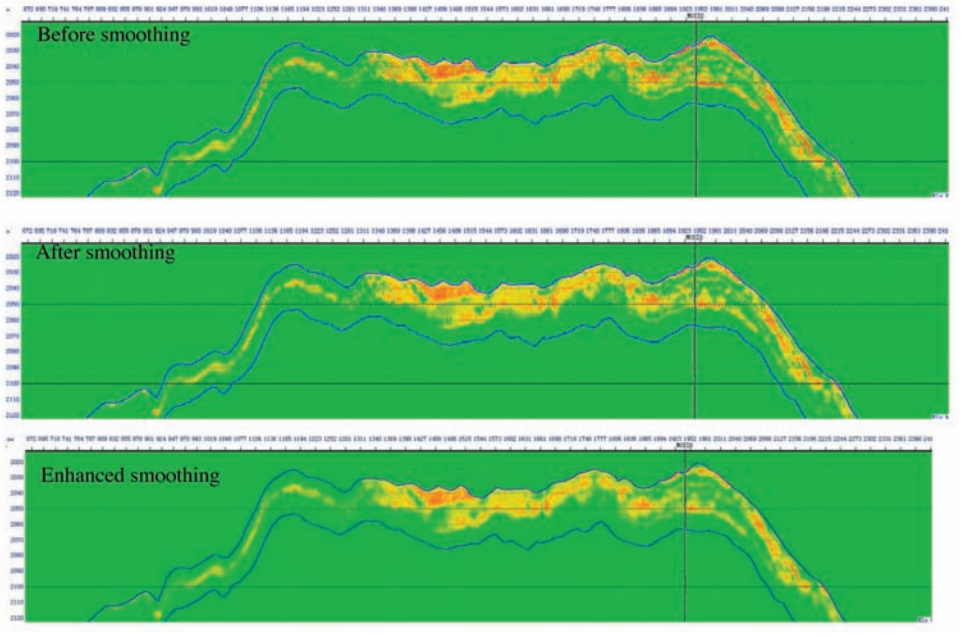

Fig. 13. The 2D crossing-MX8 seismic inversion sections of the porosity before smoothing, after smoothing, and with an enhanced smoothing.

the gas accumulations are located in the two zones in concentration, the upper and the lower gas zones. The results are in good agreement with the conclusions from the relevant petroleum geology studies on this area. In addition, the inversion results also agrees with the gas production report data of the most wells, such as the well MX203 where gas is produced at the upper part and water is produced at the lower part for the formation, and the well MX8 with the high gas production rate.

As is shown in Figs. 16 and 17, in the two 2D crossing-well sections which are extracted from the 3D rock physics inversion data volume, the inversion results are compared with the log interpretation results and gas production test data.

Fig. 16 shows the results crossing well MX13. It is obvious the porosity from seismic inversion is generally in good agreement with the porosity from log interpretation and serial core measurements. The seismic inversion effectively identifies the most high-quality reservoirs in the middle part of the

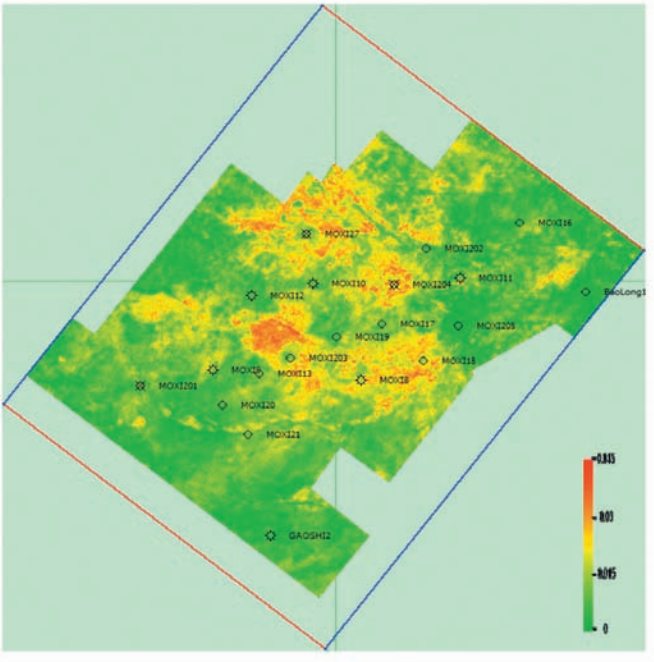

Fig. 14. Inversion results of the reservoir average porosity in the work area.

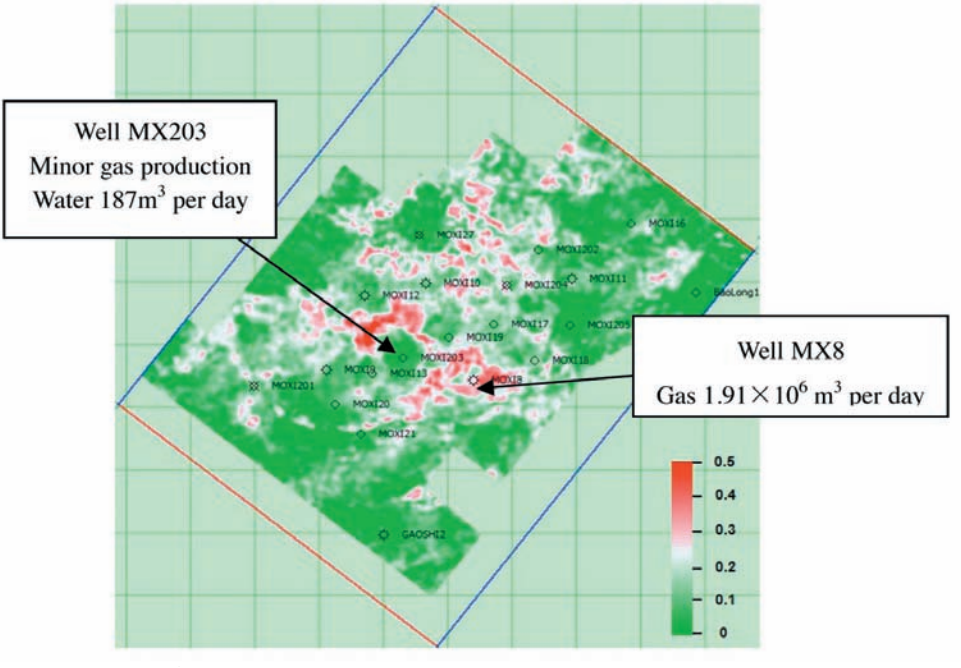

Fig. 15. Inversion results of the reservoir average gas saturation in the work area.

target formation. The gas saturation results show that in the target formation around well MX13 there is high gas-bearing potential, which is consistent with the gas production data (the daily gas production from the target formation at this well reaches 1.2884×10^6 m^3 per day), and those structural low positions on the same section display high possibility of water-bearing reservoirs. The inversion results preliminarily show the possibility of a direct seismic identification of gas-water contact controlled by structures. Fig. 17 shows the inversion results crossing well MX17. The inversion results precisely identify the three thin gas layers which are also identified in log interpretation results, the total gas production rate of which are 0.532×10^6 m^3 per day.

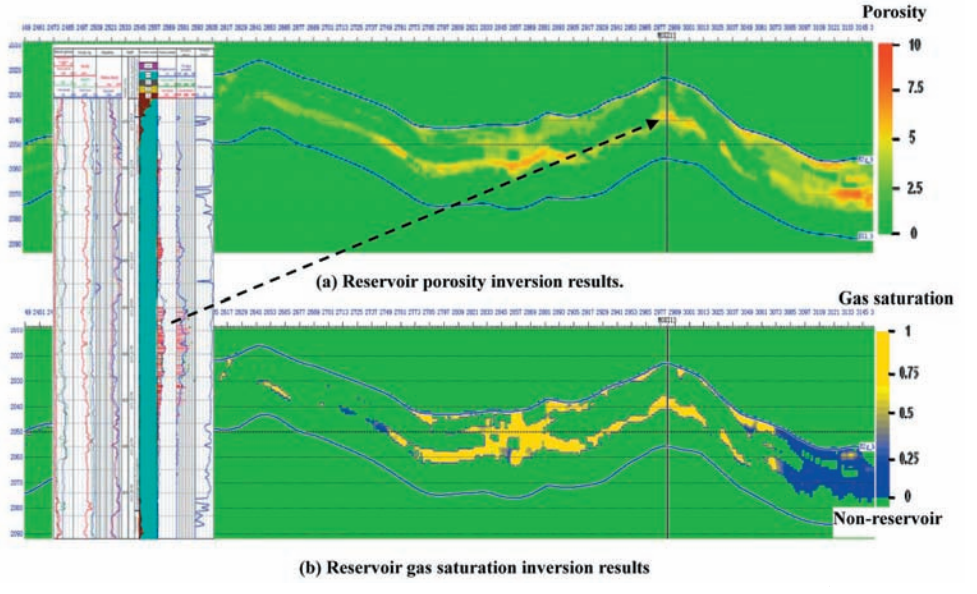

Fig. 16. Inversion results crossing-well MX13 of reservoir porosity and gas saturation. (a) Reservoir porosity inversion results. (b) Reservoir gas saturation inversion results.

CONCLUSIONS

Regarding the strong heterogeneity characteristics of carbonate reservoirs, this paper analyzes the mineral components, pore structures and fluid substitution of reservoir rocks to develop the multi-scale rock physics models. Based on multi-scale rock physics modeling, an industrial technical workflow of rock physics inversion on reservoir and fluid parameters is presented for the large-area 3D seismic survey.

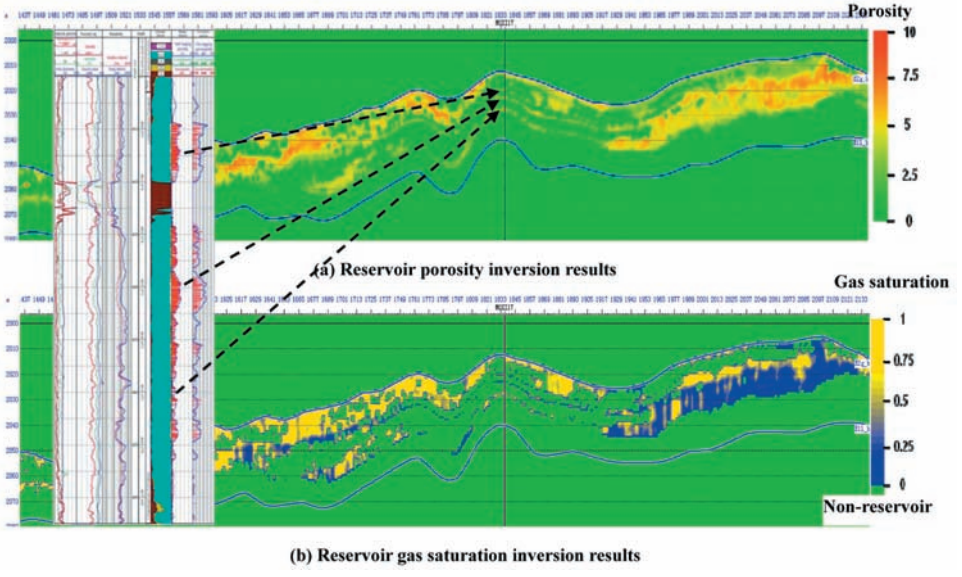

Fig. 17. Inversion results crossing-well MX17 of reservoir porosity and gas saturation. (a) Reservoir porosity inversion results. (b) Reservoir gas saturation inversion results.

Log data analysis and re-interpretation are performed to calibrate the single-well rock physics model and relevant template. The fluid/hydrocarbon sensitivity of rock physics parameters are analyzed at the scales of sonic log and ultrasonic laboratory measurements. The results show that the fluid sensitivity of each rock parameter declines notably as the rock porosity decreases. However, the sensitivity sequence of the parameters are almost unchanged with porosity. The general sensitivity sequence of the rock parameters is basically consistent between the two scales, however the sensitivity for the same parameter varies slightly between. Based on the multi-scale sensitivity analysis, the parameters $\lambda\rho$ and λ which are the most sensitive to the fluid changes are sorted out.

To describe the general geological characteristics of the target formation, the modeling results from each single well are optimized to develop the standard rock physics model/template of the large work area. By use of the crossing-well 2D seismic inversion tests, the data volume of 3D rock physics model are produced for the large 3D area, which is combined with the pre-stack seismic inversion to estimate the reservoir porosity and gas saturation. The data volume

of inversion results are smoothed by the smoothing matrix methods. The inversion results are compared with the log data interpretation and gas production test reports at the target formation, and are validated to be in good agreement with the actual porosity in in-situ rocks and the gas production rates.

Based on the rock physics analysis, this paper presents the industrial technical workflow for seismic quantitative prediction of reservoir and fluid parameters. It is successfully applied to the tight dolomite reservoirs of MX area in west China. By considering the difference in geological characteristics, reservoir types and fluid distribution patterns from different work area, the varied lithology, pore structures and fluids have to be analyzed according to the realities of in-situ rocks, to ensure the applicability and accuracy of the developed rock physics model. Calibrations have to be made according to the experimental measurements, log observations and seismic data, so that the seismic rock physics inversion methods can be applied efficiently.

ACKNOWLEDGEMENTS

This work is supported by the Distinguished Professor Program of Jiangsu Province, China, the Natural Science Foundation of China (41204096) and the National Science and Technology Major Project of China (2011ZX05013-001).

REFERENCES

Avseth, P., Mukerji, T. and Mavko, G., 2005. Quantitative Seismic Interpretation: Applying Rock Physics Tools to Reduce Interpretation Risk. Cambridge University Press, Cambridge.

Ba, J., Carcione, J.M. and Nie, J.X., 2011. Biot-Rayleigh theory of wave propagation in double-porosity media. J. Geophys. Res., 116(B6): B06202.

Ba, J., Carcione, J.M., Cao, H., Da, Q.Z., Yuan, Z.Y. and Lu, M.H., 2012. Velocity dispersion and attenuation of P waves in partially-saturated rocks: Wave propagation equations in double-porosity medium. Chin. J. Geophys., 55: 219-231.

Ba, J., Cao, H., Carcione, J.M., Tang, G., Yan, X., Sun, W. and Nie, J., 2013a. Multiscale rock-physics templates for gas detection in carbonate reservoirs. J. Appl. Geophys., 93: 77-82.

Ba, J., Yan, X.Y., Chen, Z.Y., Xu, G.C., Bian, C.S., Cao, H., Yao, F.C. and Sun, W.T., 2013b. Rock physics model and gas saturation inversion for heterogeneous gas reservoirs. Chin. J. Geophys., 56: 1696-1706.

Ba, J., Zhao, J., Carcione, J.M. and Huang, X., 2016. Compressional wave dispersion due to rock matrix stiffening by clay squirt flow. Geophys. Res. Lett., 43: 6186-6195.

Berryman, J.G., 1980. Long-wavelength propagation in composite elastic media II. Ellipsoidal inclusions. J. Acoust. Soc. Am., 68: 1820-1831.

Biot, M.A., 1956. Theory of propagation of elastic waves in a fluid-saturated porous solid: I. Low-frequency range. J. Acoust. Soc. Am., 28: 168-178.

Biot, M.A., 1962. Mechanics of deformation and acoustic propagation in porous media. J. Appl. Phys., 33: 1482-1498.

Carcione. J.M. and Avseth, P., 2015. Rock-physics templates for clay-rich source rocks. Geophysics, 80: D481-D500.

Caspari, E., Müller, T.M. and Gurevich, B., 2011. Time-lapse sonic logs reveal patchy CO_2 saturation in-situ. Geophys. Res. Lett., 38: L13301.

Chi, X.G. and Han, D.H., 2009. Lithology and fluid differentiation using a rock physics template. The Leading Edge, 28: 60-65.

Deng, J.X., Wang, H., Zhou, H., Liu, Z.H., Song, L.T. and Wang, X.B., 2015. Microtexture, seismic rock physical properties and modeling of Longmaxi formation shale. Chin. J. Geophys., 58: 2123-2136.

Dvorkin, J. and Nur, A., 1993. Dynamic poroelasticity: A unified model with the squirt and the Biot mechanisms. Geophysics, 58: 524-533.

Gassmann, F., 1951. Über die Elastizität poröser Medien: Vier. der Natur. Gesellschaft in Zürich, 96: 1-23.

Gurevich, B., Makarynska, D., Paula, O.B.D. and Pervukhina, M., 2010. A simple model for squirt-flow dispersion and attenuation in fluid-saturated granular rocks. Geophysics, 75: N109-N120.

He, H.B., You, J. and Chen, K.Y., 2011. Gas sand distribution prediction by prestack elastic inversion based on rock physics modeling and analysis. Appl. Geophys., 8: 197-205.

Jin, M.D., Zeng, W., Tan, X.C., Li, L., Li, Z.Y., Luo, B., Zhang J.L. and Liu, J.W., 2014. Characteristics and controlling factors of beach-controlled karst reservoirs in Cambrian Longwangmiao Formation, Moxi-Gaoshiti area, Sichuan Basin, NW China. Petrol. Explor. Develop., 41: 712-723.

Liu, Y.Q., 2014. Construction and Application of Fluid Identification Factors based on Porous Media. Jilin University, Changchun.

Lv, Q.B. and Sun, Z.X., 2012. Application of rock physics chart to quantitative reservoir interpretation. Progr. Geophys. (in Chinese), 27: 610-618.

Mavko, G. and Nur, A., 1975. Melt squirt in the asthenosphere. J. Geophys. Res., 80: 1444-1448.

Nicolás-López, R. and Valdiviezo-Mijangos, O.C., 2016. Rock physics templates for integrated analysis of shales considering their mineralogy, organic matter and pore fluids. J. Petrol. Sci. Engineer., 137: 33-41.

Ødegaard, E. and Avseth, P., 2004. Well log and seismic data analysis using rock physics templates. First Break, 22: 37-43.

Papageorgiou, G. and Chapman, M., 2015. Multifluid squirt flow and hysteresis effects on the bulk modulus-water saturation relationship. Geophys. J. Internat., 203: 814-817.

Pride, S.R. and Berryman, J.G., 2003. Linear dynamics of double-porosity dual-permeability materials. I: Governing equations and acoustic attenuation. Phys. Rev. E, 68: 036603.

Russell, B.H., Hedlin, K., Hilterman, F.J. and Lines, L.R., 2003. Fluid property discrimination with AVO: A Biot-Gassmann perspective. Geophysics, 68: 29-39.

Russell, B.H., Gray, D. and Hampson, D.P., 2011. Linearized AVO and poroelasticity. Geophysics 76(3): C19-C29.

Sun, W.T., Ba, J., Müller, T.M., Carcione, J.M. and Cao, H., 2014. Comparison of P-wave attenuation models of wave-induced flow. Geophys. Prosp., 63: 378-390.

Tang, J.W., 2008. Discussion on several issues about seismic rock physics. Geophys. Prosp. Petrol., 47: 398-404.

Tang, S.W., 2011. Research of image processing methods and technology in seismic interpretation. Ph.D. thesis. Northeast Petroleum University, Daqing.

Vinci, C., Renner, J. and Steeb, H., 2014. On attenuation of seismic waves associated with flow in fractures. Geophys. Res. Lett., 41: 7515-7523.

White, J.E., 1975. Computed seismic speeds and attenuation in rocks with partial gas saturation. Geophysics, 40: 224-232.

Yang, X.F., Wang, X.Z., Yang, Y.M., Li, X.Y., Jiang, N., Xie, J.R. and Luo, W.J., 2015. Diagenesis of the dolomite reservoir in lower Cambrian Longwangmiao formation in central Sichuan basin. Geol. Sci. Technol. Info., 34: 35-41.

Yin, X.Y., Zhang, S.X., Zhang, F.C. and Hao, Q.Y., 2010. Utilizing Russell Approximation based elastic wave impedance inversion to conduct reservoir description and fluid identification. Oil Geophys. Prosp., 45: 373-380.

Yin, X.Y., Zhang, S.X. and Zhang, F., 2013. Delicate construction of fluid factor and its application based on two-phase media theory. Progr. Geophys. (in Chinese), 28: 2911-2918.

Yin, X.Y., Cao, D.P., Wang, P.L. and Zong, Z.Y., 2014. Research progress of fluid discrimination with prestack seismic inversion. OGP, 49: 22-34.

Yin, X.Y., Zong, Z.Y. and Wu, G.C., 2015. Research on seismic fluid identification driven by rock physics. Sci. China: Earth Sci., 58: 159-171.

Yu, H., Ba, J., Carcione, J.M., Li, J.S., Tang, G., Zhang, X.Y., He, X.Z. and Ouyang, H., 2014. Rock physics modeling of heterogeneous carbonate reservoirs: porosity estimation and hydrocarbon detection. Appl. Geophys., 11: 9-22.

Zhang, Z., Yin, X.Y. and Hao, Q.Y., 2014. Frequency-dependent fluid identification method based on AVO inversion. Chin. J. Geophys., 57: 4171-4184.

Zhang, G.Z., Chen, J.J., Chen, H.Z., Zhang, J.Q. and Yin, X.Y., 2015. Quantitative interpretation of Carbonate gas reservoir based on rock physics template. J. Jilin Univ.: Earth Sci. Ed., 45: 630-638.

Zong, Z.Y., Yin, X.Y. and Zhang, F.C., 2011. Elastic impedance Bayesian inversion for lame parameters extracting. OGP, 46: 598-604.

Zong, Z.Y., Yin, X.Y. and Wu, G.C., 2012. Fluid identification method based on compressional and shear modulus direct inversion. Chin. J. Geophys., 55: 284-292.

Zong, Z.Y., Yin, X.Y. and Wu, G.C., 2015. Geofluid discrimination incorporating poroelasticity and seismic reflection inversion. Surv. Geophys., 36: 659-681.